Investigating 2,2‘-Bipyridine-3,3‘-diol as a Microenvironment-Sensitive Probe: Its Binding to Cyclodextrins and Human Serum Albumin

ARTICLE *in* THE JOURNAL OF PHYSICAL CHEMISTRY B · SEPTEMBER 2007

Impact Factor: 3.3 · DOI: 10.1021/jp073480q · Source: PubMed

1 AUTHOR:

Osama Kamal Abou-Zied
Sultan Qaboos University
50 PUBLICATIONS **951** CITATIONS

SEE PROFILE

Investigating 2,2′-Bipyridine-3,3′-diol as a Microenvironment-Sensitive Probe: Its Binding to Cyclodextrins and Human Serum Albumin

Osama K. Abou-Zied*

Department of Chemistry, Faculty of Science, Sultan Qaboos University, P.O. Box 36, Postal Code 123, Muscat, Sultanate of Oman

Received: May 7, 2007; In Final Form: June 11, 2007

The 2,2′-bipyridine-3,3′-diol molecule ($BP(OH)_2$) was investigated as a potential photophysical probe in inclusion and biological studies. Binding of $BP(OH)_2$ to cyclodextrins (CDs) and human serum albumin (HSA) was studied by following the changes in its absorption and fluorescence spectra. The stoichiometric ratios and binding constants of the complexes were deduced by fitting the changes in the spectral intensity to binding isotherms. The stoichiometric ratio in the $BP(OH)_2$/(α-CD) complex is dominated by 1:2, whereas in all other CDs and in HSA this ratio is 1:1. The structure of the $BP(OH)_2$:$(\alpha\text{-CD})_2$ complex, calculated using ab initio methods, indicates that the inclusion of the $BP(OH)_2$ molecule is axial and centered between the two cavities of α-CD with van der Waals and electrostatic interactions dominating the binding. Analysis of these results along with the inclusion results of $BP(OH)_2$ in *β*-CD, methyl-*β*-CD, 2,6-di-*O*-methyl-*β*-CD, and *γ*-CD shows that absorption and fluorescence of $BP(OH)_2$ are very sensitive to the change in the cavity size of CD and its hydrophobicity. This change is reflected in the form of a decrease in the intensity of the absorption peaks of the $BP(OH)_2$/water complex in the region 400−450 nm and a red shift in the fluorescence peak as the cavity size decreases and its hydrophobicity increases. Binding of $BP(OH)_2$ as a probe ligand to HSA, a prototype protein, reflects the hydrophobic interior of HSA in a similar manner. The spectral changes indicate that $BP(OH)_2$ binds in the hydrophobic cavity of HSA's subdomain IIA. The results presented here show that $BP(OH)_2$ can be used in binding sites and biological systems as a microenvironment-sensitive probe.

Introduction

Extrinsic fluorescent probes are widely used for the investigation of physicochemical, biochemical, and biological systems owing to the strong influence of the surrounding medium on their fluorescence emission.[1] These probes are highly sensitive to the environmental changes which are reflected in their fluorescence intensity and/or spectral position. A very important criterion in the choice of a probe is its sensitivity to a particular property of the microenvironment in which it is located (e.g., polarity, acidity, etc.). There has been an increased interest recently in studying a class of molecules which possess one or more hydrogen bonds in their structure. These molecules can be photoinduced to tautomerize in the excited state. Due to their extreme sensitivity to solvent polarity and hydrogen bonding with protic solvents, some of these molecules have been suggested as probes for the study of protein conformation and binding sites.[2−5] We propose here one such molecule which is 2,2′-bipyridine-3,3′-diol ($BP(OH)_2$) as a very sensitive probe to microenvironment change by examining its steady-state spectra in different environments.

The photoinduced excited-state intramolecular double proton transfer (ESIDPT) in $BP(OH)_2$, shown in Figure 1, has been extensively studied both experimentally[6−17] and theoretically.[18−21] Electro-optical absorption and emission and calculated excited-state dipole moments show that the dipole moments of the di-enol (DE) and the di-keto (DK) tautomers are negligible, whereas the dipole moment is 4.0−4.9 D for the mono-keto (MK) tautomer.[11,12] At room temperature, $BP(OH)_2$ absorbs in the region of 350 nm yet fluoresces strongly in the green. Quantum yields of fluorescence in the order of 0.2−0.4 were observed in different solvents at room temperature with lifetimes of a few nanoseconds.[6−10] Comparing the absorption and emission properties of $BP(OH)_2$ with related systems possessing only one hydrogen bond reveals that the second hydroxyl group is essential to the observation of the strong green emission. This emission is due to fluorescence from the DK tautomer after an efficient ESIDPT process. Both concerted and stepwise mechanisms were proposed for the double proton transfer in $BP(OH)_2$, as illustrated in Figure 1.[13−21] The $BP(OH)_2$ molecule is also planar in crystalline form[22] and is expected to retain its planarity in solutions of non-interacting solvents because of the two strong intramolecular hydrogen bonds.

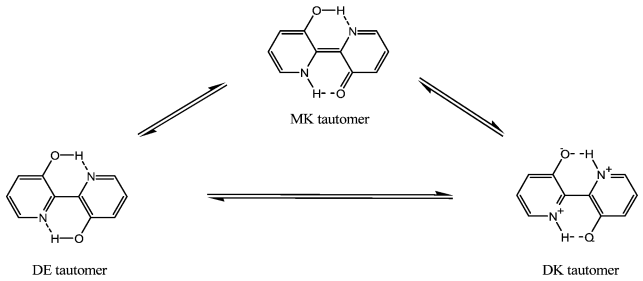

Figure 1. Tautomerization in $BP(OH)_2$ showing stepwise and concerted mechanisms.

We have recently reported the steady-state spectra of $BP(OH)_2$ in solvents of varying polarity and hydrogen-bonding capability, and in binary mixtures of 1,4-dioxane/water.[23] Unique absorption due to water solvation was observed in the region 400−450 nm. A large blue shift in the fluorescence band due

* Phone: (+968) 2414-1468. Fax: (+968) 2414-1469. E-mail: abouzied@squ.edu.om.

10.1021/jp073480q CCC: $37.00
Published on Web 07/27/2007

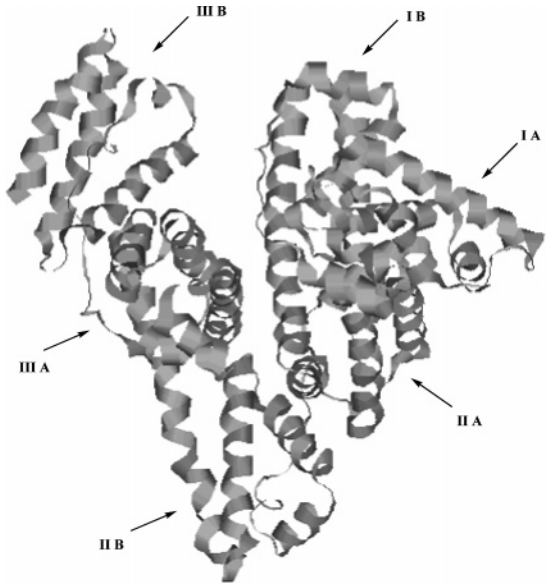

Figure 2. Crystal structure of HSA and the locations of domain-binding sites. The structure was obtained from the Protein Data Bank (ID code 1ha2).

to intermolecular hydrogen bonding was observed in polar, protic solvents. The shift increases with increasing solvent polarity. We also studied $BP(OH)_2$ in several cyclodextrins (CDs) in order to examine the effect of hydrophobic environments on its absorption and fluorescence spectra.[24] Experiments using β-CD, 2,6-di-*O*-methyl-β-CD (DMβ-CD), and γ-CD as caging media have shown that decreasing the cavity size and increasing its hydrophobicity cause a large reduction in the absorption features in the region 400−450 nm and a large red shift in the fluorescence peak of $BP(OH)_2$. We interpreted the results to be due to the decrease in water accessibility inside the CD cavities. The results led us to propose $BP(OH)_2$ as a possible water sensor in biological systems.

In continuation of the above study, we examine in this paper the behavior of $BP(OH)_2$ in the smaller cavity of α-CD. We compare the caging effect of α-CD with our previous results on the effects of other CDs,[24] and we also add the caging effect of methyl-β-CD (Mβ-CD) in order to draw a general comparison in relation to the cavity size and hydrophobicity of the CDs. We then use $BP(OH)_2$ as a probe ligand and human serum albumin (HSA) as a prototype protein in order to test the applicability of $BP(OH)_2$ as a biological probe. HSA constitutes approximately half of the protein found in human blood.[25] It recognizes a wide variety of agents and transports these agents in the blood stream. The X-ray crystal structure of HSA[26,27] (Figure 2) indicates an asymmetric heart-shaped molecule that can be roughly described as an equilateral triangle. The two heart lobes contain the molecule's hydrophobic binding sites, while the outside of the molecule contains most of the polar groups. As shown in Figure 2, the binding sites in HSA are classified into three domains. Each domain is a product of two subdomains, A and B, with common structural motifs. The study of the $BP(OH)_2$/HSA system should be useful for understanding molecular recognition in protein/ligand complexes on a molecular level which is crucial to biological function.[28]

Experimental and Theoretical Methods

$BP(OH)_2$ (98%) was obtained from Aldrich and was used without further purification. α-CD (≥98%) and Mβ-CD (≥97%) were purchased from Fluka and used as supplied. Deionized water (Millipore) was used in all preparations and dilutions in CDs. The buffer used was 50 mM sodium phosphate buffer, pH 7.0, and it was obtained from Aldrich. HSA (essentially fatty acid free) was purchased from Sigma. The concentration of HSA in the buffer was determined spectrophotometrically by using $\epsilon_{280} = 36.6\ mM^{-1}\ cm^{-1}$.[29] The concentration of $BP(OH)_2$ in all solvents, including the buffer, was ≈0.01 mM. Complexes of $BP(OH)_2$ with α-CD, Mβ-CD, and HSA were prepared and allowed to equilibrate for 2 h before taking the measurements. Measurements were repeated after 12 h, and no significant differences were detected.

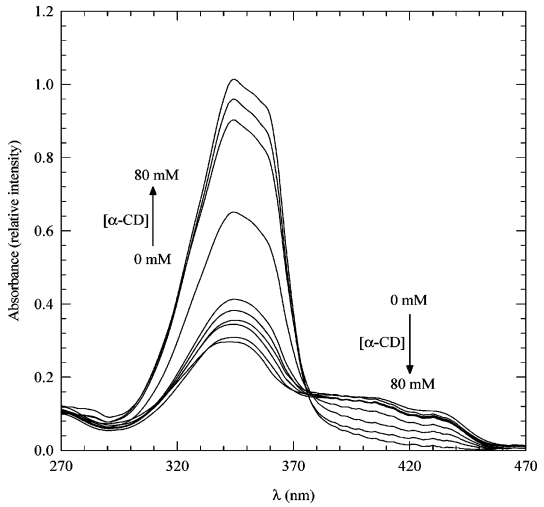

Figure 3. Absorption spectra of $BP(OH)_2$ in aqueous solutions with varying concentrations of α-CD.

Absorption spectra were obtained with an HP 845x Diode Array spectrophotometer. Fluorescence spectra were recorded on a Shimadzu RF-5301 PC spectrofluorophotometer. In all of the experiments, samples were contained in a 1 cm path length quartz cell and the measurements were conducted at 23 ± 1 °C.

Geometry optimization of the $BP(OH)_2$/α-CD complex was carried out using the GAMESS program.[30]

Results and Discussion

Absorption and Fluorescence Spectra of $BP(OH)_2$ in α-CD. The absorption spectra of $BP(OH)_2$ in aqueous solutions with varying concentrations of α-CD are shown in Figure 3 for the spectral region from 270 to 470 nm. The peak at 344 nm represents the transition to the lowest $^1(\pi,\pi^*)$ state.[6] Our previous study of $BP(OH)_2$ in different solvents shows that the absorbance intensity in the 400−450 nm region only appears in water and gains its strength at the expense of that at 344 nm.[23,24] It was suggested that water stabilizes the DK tautomer in the ground state.[20,31]

The spectra in Figure 3 show that, as the α-CD concentration increases, the intensity of the peak at 344 nm increases with a concomitant decrease in the intensity of the two peaks in the region 400−450 nm. This trend is due to the caging effect of the α-CD cavity on the guest molecule. Upon complexation, the $BP(OH)_2$ molecule experiences shielding from the water molecules outside the CD cavity. Hence, the decrease in the absorbance intensity in the region 400−450 nm is a manifestation of how deep the $BP(OH)_2$ molecule is buried inside the CD cavity.

The fluorescence spectra of $BP(OH)_2$ were recorded in aqueous solutions with varying α-CD concentrations and are

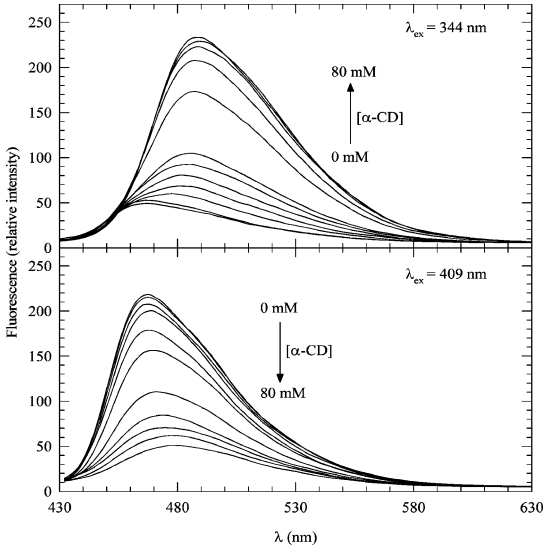

Figure 4. Fluorescence spectra of BP(OH)$_2$ in aqueous solutions with varying concentrations of α-CD at two different excitation wavelengths, as indicated.

shown in Figure 4. Fluorescence in BP(OH)$_2$ is due to the DK tautomer after ESIDPT.[19,23] Increasing the α-CD concentration leads to a red shift of the fluorescence peak resulting from excitation at 344 nm with an increase in the intensity. On the other hand, the fluorescence peak resulting from excitation at 409 nm shows a decrease in the intensity with a small red shift. The change in intensity upon excitation at 344 and 409 nm is well-correlated with the change in the corresponding intensities in the absorption spectra as a function of [α-CD] (see Figure 3). The red shift in the fluorescence peak is due to a change in environment from high to low polarity.[23] The latter is experienced as a result of the caging effect of the CD cavity. The changes in intensity and spectral position of the fluorescence peak confirm the more hydrophobic nature of the environment experienced by the BP(OH)$_2$ molecule as the α-CD concentration increases.

Stoichiometric Ratio and Binding Constant of the BP(OH)$_2$/α-CD Complex. The stoichiometric ratio and the binding constant of the BP(OH)$_2$/α-CD complex were estimated from the Benesi−Hildebrand (BH) double-reciprocal plots.[24,32−34] The change in the absorption intensity is correlated to the initial CD concentration according to

$$\frac{1}{A - A_0} = \frac{1}{(\epsilon_c - \epsilon_0)[N]_0} + \frac{1}{(\epsilon_c - \epsilon_0)[N]_0 K[CD]_0^n} \quad (1)$$

where A and A_0 are the absorbance per centimeter of BP(OH)$_2$ aqueous solution in the presence and absence, respectively, of CD; ϵ_c and ϵ_0 are the molar absorption coefficients of the BP(OH)$_2$/CD complex and BP(OH)$_2$, respectively; $[N]_0$ is the initial concentration of BP(OH)$_2$; $[CD]_0$ is the initial concentration of CD; n represents the stoichiometry of the equilibrium reaction in relation to CD; and K is the equilibrium constant for the formation of BP(OH)$_2$/CD. Since the concentration of CD is much higher than that of BP(OH)$_2$, $[CD]_0$ is assumed constant before and after complexation.

Equation 1 can be modified to reflect the changes in the fluorescence intensity according to[24,33,34]

$$\frac{1}{F - F_0} = \frac{1}{F_c - F_0} + \frac{1}{(F_c - F_0)K[CD]_0^n} \quad (2)$$

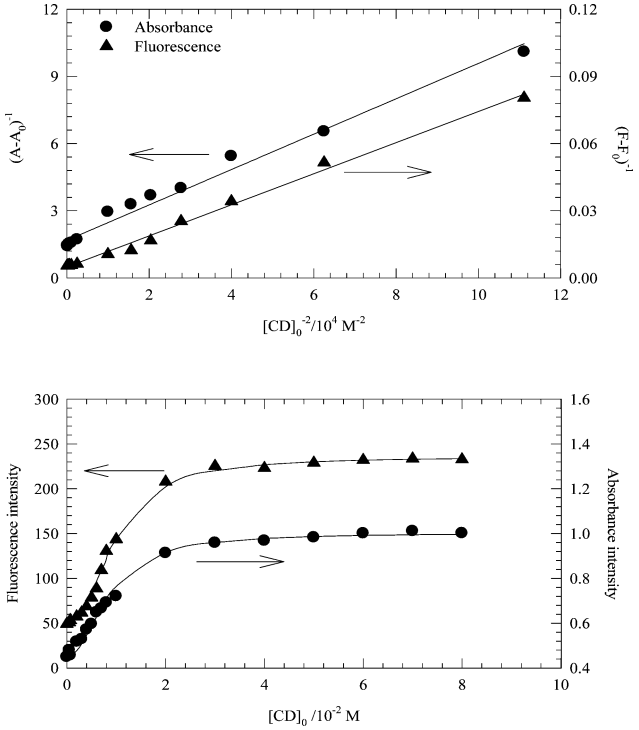

Figure 5. Upper panel: BH double-reciprocal plots (eqs 1 and 2) using the changes in absorbance at 344 nm and fluorescence ($\lambda_{ex} = 344$ nm) for the BP(OH)$_2$ molecule complexed with α-CD. Lower panel: variation of absorbance (at 344 nm) and fluorescence ($\lambda_{ex} = 344$ nm) intensities of the BP(OH)$_2$ molecule complexed with α-CD. The solid lines are the best NLR fits using eq 3 for $n = 2$.

where F and F_0 are the fluorescence intensities of BP(OH)$_2$ aqueous solution in the presence and absence, respectively, of CD and F_c is the intensity due to the BP(OH)$_2$/CD complex only.

Thus, a plot of $(A - A_0)^{-1}$ or $(F - F_0)^{-1}$ versus $[CD]^{-n}$ should yield a straight line for the correct stoichiometry (n). Typical double-reciprocal plots are shown in Figure 5 for the BP(OH)$_2$/α-CD complex. As shown in the figure, a straight line is obtained for each case when $n = 2$. No linear plot was observed for other values of n. These results suggest that the stoichiometry of the BP(OH)$_2$/CD complex is dominated by 1:2 (BP(OH)$_2$:(α-CD)$_2$).

The equilibrium constant for the complex formation was estimated from the slope and intercept of the BH plot and used as an initial guess in an iterative nonlinear regression (NLR) fit using the following equation:[24,33,34]

$$I = \frac{I_0 + I_c K[CD]_0^n}{1 + K[CD]_0^n} \quad (3)$$

where I, I_0, and I_c represent the fluorescence or the absorption intensities for the same species as in eqs 1 and 2.

More accurate K values are usually obtained from NLR fits than those estimated from double-reciprocal plots.[33,35,36] Equation 3 was found to correctly fit the experimental data when $n = 2$, confirming the stoichiometry of the complex. The NLR fits are displayed in Figure 5, and the estimated K values from absorption and fluorescence are $(11.10 \pm 1.0) \times 10^3$ and $(10.30 \pm 0.8) \times 10^3$ M^{-2}, respectively.

The formation of a 1:2 inclusion complex in BP(OH)$_2$:(α-CD)$_2$ follows the following stepwise equilibrium mechanism:

$$BP(OH)_2 + \alpha\text{-CD} \overset{K_{11}}{\rightleftharpoons} BP(OH)_2{:}(\alpha\text{-CD}) \quad (4)$$

$$BP(OH)_2{:}(\alpha\text{-CD}) + \alpha\text{-CD} \overset{K_{12}}{\rightleftharpoons} BP(OH)_2{:}(\alpha\text{-CD})_2 \quad (5)$$

The measured absorbance in the case of the $BP(OH)_2$/α-CD mixture in a 1 cm path length is the sum of the absorbance of free (uncomplexed) $BP(OH)_2$, $BP(OH)_2$:(α-CD), and $BP(OH)_2$:$(\alpha\text{-CD})_2$ according to

$$A = \epsilon_0[N] + \epsilon_{11}[N{:}CD] + \epsilon_{12}[N{:}(CD)_2] \quad (6)$$

where ϵ_0, ϵ_{11}, and ϵ_{12} are the molar extinction coefficients of free $BP(OH)_2$, $BP(OH)_2$:(α-CD), and $BP(OH)_2$:$(\alpha\text{-CD})_2$, respectively. [N], [N:CD], and [N:$(CD)_2$] are the concentrations of free $BP(OH)_2$, 1:1 complex, and 1:2 complex, respectively. On the basis of the assumption that [CD] ≫ [$BP(OH)_2$], eq 6 can be rewritten as[33,37]

$$A = \frac{\epsilon_0[N]_0 + \epsilon_{11}[N]_0K_{11}[CD]_0 + \epsilon_{12}[N]_0K_{11}K_{12}[CD]_0^2}{1 + K_{11}[CD]_0 + K_{11}K_{12}[CD]_0^2} \quad (7)$$

Equation 7 is equivalent to eq 3 but details the different contributions from each species according to the reactions in eqs 4 and 5, with $K = K_{11}K_{12}$. From the absorbance measurements, ϵ_0 was calculated to be equal to 5890 M^{-1} cm^{-1} at 344 nm. Equation 7 can thus be fitted to the measured absorbance at 344 nm for different concentrations of α-CD using the NLR algorithm. The results of the fit give $\epsilon_{11} = 9502$ M^{-1} cm^{-1}, $\epsilon_{12} = 16\,627$ M^{-1} cm^{-1}, $K_{11} = 60$ M^{-1}, and $K_{12} = 185$ M^{-1}. The larger value of K_{12} compared to that of K_{11} indicates that the addition of the second α-CD molecule adds more stability to the overall complex through interaction with $BP(OH)_2$ and the first α-CD.

Structure of the $BP(OH)_2$:$(\alpha\text{-CD})_2$ Complex. The study of encapsulation of guest molecules by CDs has been severely limited theoretically owing to the large molecular size of the whole system. Most of these investigations are restricted to semiempirical methods[38,39] or empirical force fields[40−43] in order to reduce computational costs and time. The present system is very large (274 atoms) due to the high stoichiometry of the $BP(OH)_2$:$(\alpha\text{-CD})_2$ complex.

The structure of $BP(OH)_2$:$(\alpha\text{-CD})_2$ was first calculated using AM1 and PM3 semiempirical methods with fully unconstrained geometry optimization. The structural parameters known from the X-ray studies were used as a starting point for α-CD[44] and $BP(OH)_2$.[22] The $BP(OH)_2$ molecule was introduced inside the two α-CD cavities with the two larger, secondary-hydroxy rims of CDs facing each other and capping the $BP(OH)_2$ molecule. The complex was allowed to optimize with no restrictions.

The minimum-energy conformations found in the search using both AM1 and PM3 indicate that the $BP(OH)_2$ molecule stayed inside the two CDs and was shared equally by the two cavities. The structures calculated by both semiempirical methods indicate also that there is a deviation of 54° between the planes of the two aromatic rings of $BP(OH)_2$. Furthermore, the hydrogen bond distances between the hydroxyl hydrogen and the N-heteroatom in each of the hydrogen-bonding centers of $BP(OH)_2$ are calculated to be between 2.32 and 2.41 Å. The results reflect the poorly modeled weak intermolecular interactions such as van der Waals and hydrogen bonding by semiempirical quantum chemical methods.[45]

In order to correctly characterize the complex structure, we next used ab initio calculations. Owing to the large $BP(OH)_2$:$(\alpha\text{-CD})_2$ system, the calculations were limited to Hartree−Fock/STO-3G. The minimum-energy structure after fully unconstrained geometry optimization is depicted in Figure 6. The structure of the $BP(OH)_2$ molecule stayed planar throughout the optimization process. The intramolecular O−H···N hydrogen bonds are not perturbed as the interatomic distances between the three atoms in each hydrogen-bonding center are not appreciably modified upon encapsulation (the two H···N hydrogen bonds were calculated to be 1.66 Å).

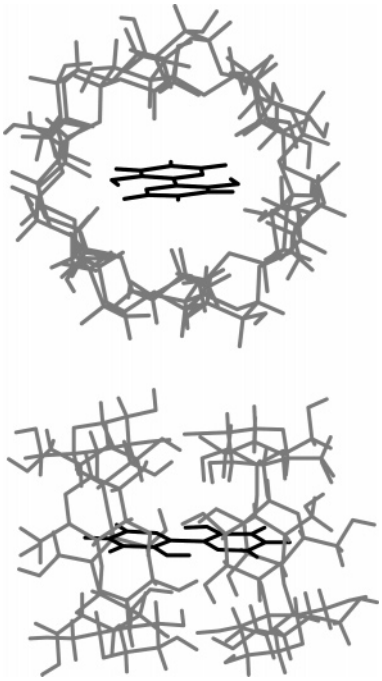

Figure 6. Structure of the most stable minimum configuration of the $BP(OH)_2$:$(\alpha\text{-CD})_2$ complex. The structure is obtained from ab initio calculations described in the text. Upper panel: top view, looking down through the primary-hydroxy rim (narrower opening) of one of the two α-CDs. Lower panel: side view.

The orientation of the $BP(OH)_2$ molecule is axial inside the CD cavities and is completely sequestered in the center between the two cavities. Analysis of the host−guest interatomic distances shows that the $BP(OH)_2$ molecule remains isolated inside the cavities and intramolecularly hydrogen-bonded in the DE form. The stability of the complex is dominated by van der Waals and electrostatic interactions. The complex structure also indicates the existence of 13 hydrogen bonds between the secondary OHs of the two α-CDs (ranging from 1.5 to 2.5 Å). These hydrogen bonds add to the stability of the 1:2 complex and may explain the larger value of K_{12} than that of K_{11}.

Comparison between the Spectra of $BP(OH)_2$ in Different CDs. In a previous paper, we reported the absorption and fluorescence spectra of $BP(OH)_2$ in γ-CD, β-CD, and DMβ-CD.[24] Here, we add to these spectra those of $BP(OH)_2$ in α-CD and we also include the spectra of one more CD (Mβ-CD). This was done in order to make a more comprehensive comparison regarding the effect of the cavity size and hydrophobicity of the CDs on the spectra of $BP(OH)_2$.

The absorption and fluorescence spectra of $BP(OH)_2$ in the five CDs are shown in Figure 7. The spectra of $BP(OH)_2$ in water and cyclohexane are also included for comparison. In all of the CDs, the intensity of the 344 nm peak in the absorption spectra is higher than that in water and the intensity in the region 400−450 nm is lower than that in water. The fluorescence spectra (normalized for clarity) show red shifts in CDs compared to fluorescence in water. The caging effect on the absorption

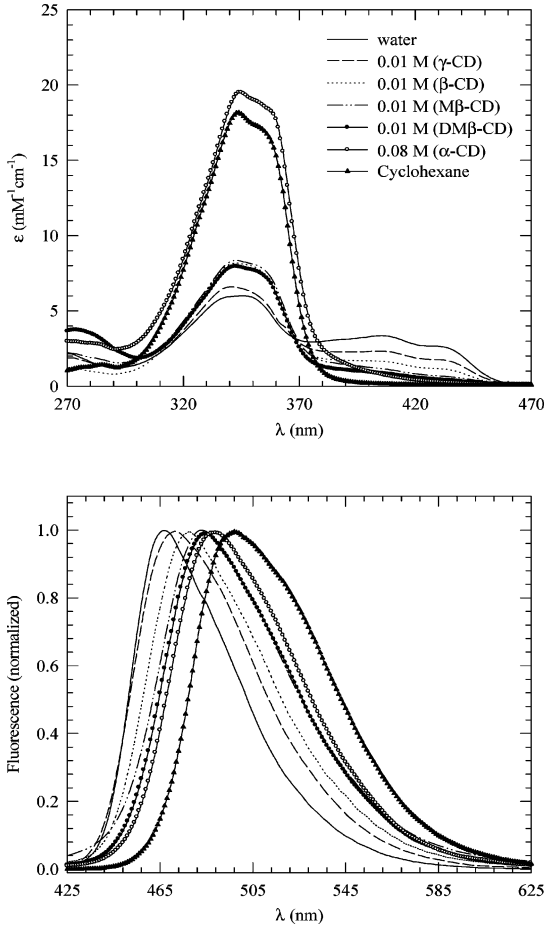

Figure 7. Absorption (upper panel) and corrected fluorescence (lower panel) spectra of $BP(OH)_2$ in water, cyclohexane, and in aqueous solutions of five CDs. The concentration of each CD used is indicated in the figure. The fluorescence spectra were normalized for clarity.

and fluorescence spectra increases as the cavity size of the CD decreases (going from γ-CD to β-CD to α-CD).[46,47] As the cavity size decreases, the guest molecule is buried inside a more hydrophobic environment where water is expelled from the cavity.[48] This process is reflected in the intensity increase of the absorption peak at 344 nm with a concomitant decrease in the intensity in the region 400−450 nm. The increase in hydrophobicity of the CD cavity is also shown as a red shift in the fluorescence peak.

The largest caging effect on the $BP(OH)_2$ molecule was observed in the 1:2 complex between $BP(OH)_2$ and α-CD. This is manifested in Figure 7 as the highest intensity of the 344 nm peak and as the lowest intensity in the region 400−450 nm. In fluorescence, the largest red shift in all CDs was observed for the $BP(OH):(\alpha\text{-CD})_2$ complex, where its fluorescence peak approaches that of $BP(OH)_2$ in cyclohexane.

The change in the cavity environment of different CDs is reflected in the binding constants of the complexes. These constants were estimated from the changes in the absorbance and fluorescence intensities as functions of CD concentrations. Table 1 summarizes the results.

β-CD, Mβ-CD, and DMβ-CD all have the same cavity diameter, but the hydrogen-bonding ability of the alcoholic hydrogens in β-CD is low compared to those of the derivatives Mβ-CD and DMβ-CD. This is because, in the former, the secondary alcoholic −OH groups at the 2- and 3-positions of the adjacent glucopyranose rings are engaged in intramolecular hydrogen bonding with each other. As a result, β-CD is less

TABLE 1: Estimated Binding Constants for $BP(OH)_2$ in Different CDs

CD	absorbance data	fluorescence data
	1:1 (K (M^{-1}))	
γ-CD	385 (±100)	335 (±80)
β-CD	860 (±95)	875 (±85)
Mβ-CD	950 (±100)	950 (±70)
DMβ-CD	1170 (±135)	1188 (±100)
	1:2 (K (M^{-2}))	
α-CD	$(11.1 \pm 1.0) \times 10^3$	$(10.3 \pm 0.8) \times 10^3$

soluble in water than its derivatives. In Mβ-CD and DMβ-CD, however, this intramolecular hydrogen bonding is destroyed due to substitution of the alcoholic protons at the 2-position with methyl groups. As a consequence, the intermolecular hydrogen-bonding ability of the alcoholic −OH group at the 3-position with water is enhanced. Substitution at the 2- and 6-positions in DMβ-CD also increases the hydrophobicity of the cavity,[48] which leads to a stronger association between $BP(OH)_2$ and DMβ-CD compared to that between $BP(OH)_2$ and β-CD and enhances more penetration of $BP(OH)_2$ inside the cavity of DMβ-CD. This is reflected in the dramatic decrease in the absorbance intensity in the region 400−450 nm for the $BP(OH)_2$:DMβ-CD complex and also the large red shift in its fluorescence peak, as shown in Figure 7.

For Mβ-CD, the methyl substitution ratio is 1.7−1.9.[49] This indicates that Mβ-CD is not mono-methylated and may carry up to two methyl groups in each sugar unit. Both absorption and fluorescence spectra of $BP(OH)_2$:Mβ-CD show a caging effect intermediate between the caging effects in $BP(OH)_2$:β-CD and $BP(OH)_2$:DMβ-CD.

The above results in different CDs show that the $BP(OH)_2$ molecule represents a potentially useful new photophysical probe for supramolecular structures, particularly those involving inclusion. The results may also suggest a method to quantify the polarity of a given CD cavity by comparing the position of the fluorescence peak with that measured in different solvents. However, such correlation is complicated for the present system by the fact that the fluorescence peak shift of $BP(OH)_2$ in different solvents proved to be a function of not only the polarity of the solvent but also its hydrogen-bonding capability.[23] For example, the fluorescence peak position was measured in methanol ($\epsilon = 32.66$, $\pi^* = 0.60$)[50] at 476 nm, whereas in acetonitrile ($\epsilon = 35.94$, $\pi^* = 0.75$)[50] it was measured at 493 nm.[23] This observation contradicts the trend observed in Figure 7 if only polarity was accounted for. Since methanol is less polar than acetonitrile, the observed blue shift in methanol must derive from intermolecular hydrogen-bonding interaction between $BP(OH)_2$ and methanol in the excited-state potential energy surface, as suggested by Marks et al.[16]

Determination of the dielectric constant inside CD nanocavities on the basis of the intensity change and shift of the absorption or fluorescence peaks of guest molecules depends on the host−guest combinations. Values ranging widely from $\epsilon = 5$ to $\epsilon = 74$ were reported.[51,52] This dispersion of the dielectric constants in CD may be explained by the size difference between the guest molecule and the cavity diameters. If the guest molecule is smaller than the CD cavity, the cavity may include water molecules together with the guest molecule. On the other hand, if the guest molecule is larger than the cavity size, only part of the guest molecule will be incorporated into the cavity, and a large moiety of the guest may be exposed to the aqueous environment. In addition, guest molecules in complexes with a stoichiometric ratio different than 1:1 will experience more of the shielding effect from the aqueous

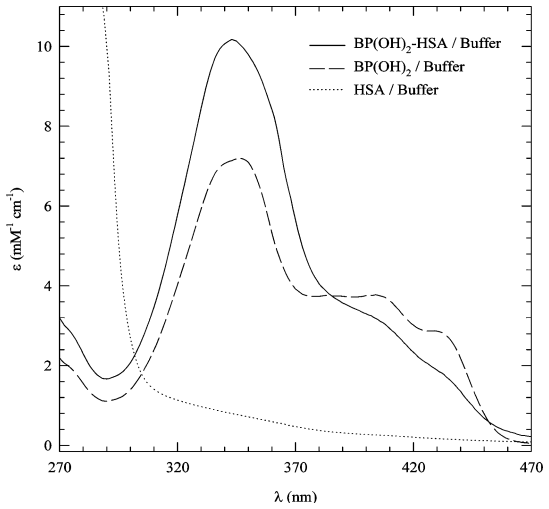

Figure 8. Absorption spectra of $BP(OH)_2$ free in buffer and in buffer containing 0.5 mM HSA. The spectrum of HSA in buffer is included for comparison.

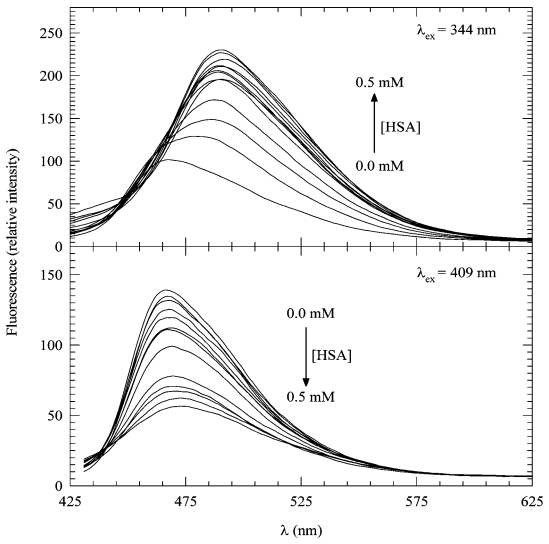

Figure 9. Fluorescence spectra of $BP(OH)_2$ free in buffer and in buffer containing different concentrations of HSA at two different excitation wavelengths, as indicated.

medium than in 1:1 complexes. The 1:2 complex of $BP(OH)_2$ in α-CD is a typical example when the spectral changes are compared with the other 1:1 complexes.

Spectra of $BP(OH)_2$ in HSA. The absorption spectra of $BP(OH)_2$ in buffer only and in buffer containing HSA are shown in Figure 8. In HSA, the absorbance in the region 400−450 nm is reduced, whereas that at 344 nm is enhanced. According to the results obtained above in CDs, the change in the absorption of $BP(OH)_2$ in HSA is due to the change in the local environment of $BP(OH)_2$ upon recognition by HSA. This confirms the binding of $BP(OH)_2$ to HSA.

The fluorescence spectra of $BP(OH)_2$ in buffer with varying concentrations of HSA are shown in Figure 9. Excitation at 344 nm results in a progressive red shift of the fluorescence peak as the HSA concentration is increased. The spectra also show an increase in the peak intensity as a function of HSA concentration. The change in the fluorescence intensity and the red shift is due to the change in the local environment of $BP(OH)_2$ upon recognition by HSA. This change confirms the binding of $BP(OH)_2$ to HSA. After excitation at 409 nm, fluorescence decreases in intensity as a function of HSA concentration which is attributed to an increase in the hydrophobic environment

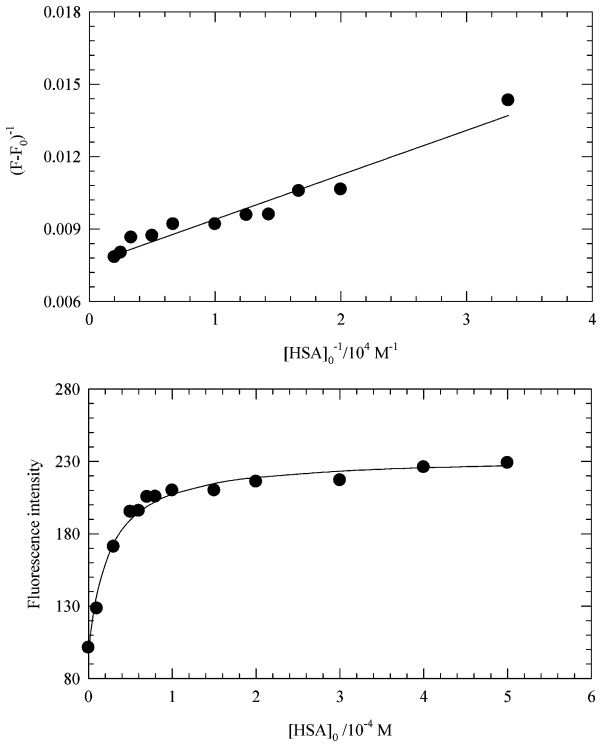

Figure 10. Upper panel: BH double-reciprocal plot (eq 2) using the change in fluorescence (λ_{ex} = 344 nm) for the $BP(OH)_2$ molecule complexed with HSA. Lower panel: variation of fluorescence (λ_{ex} = 344 nm) intensity of the $BP(OH)_2$ molecule complexed with HSA. The solid line is the best NLR fit using eq 3 for $n = 1$.

around the $BP(OH)_2$ molecule upon binding inside HSA. The binding constant of the $BP(OH)_2$/HSA complex was estimated from the fluorescence intensity change as a function of HSA concentration to be $(5 \pm 1) \times 10^4\ M^{-1}$ with a stoichiometry of 1:1. The fits using eqs 2 and 3 are shown in Figure 10.

The regions for ligand bindings to HSA are located in hydrophobic cavities in subdomains IIA and IIIA.[26] Binding site IIA is dominated by the strong hydrophobic interactions with most neutral, bulky, heterocyclic compounds. Binding site IIA is also known to bind aromatic anion molecules such as warfrin by hydrophobic interaction.[26] $BP(OH)_2$ is then expected to be bound to subdomain IIA.

The spectral changes after recognition by HSA reveal important features for $BP(OH)_2$ as a potential biological probe. The absorption peaks due to water solvation in the region 400−450 nm may act as a measure of how much $BP(OH)_2$ is shielded from water inside the HSA binding domain. Also, the progressive red shift in the fluorescence peak of the DK tautomer and the change in its intensity make $BP(OH)_2$ a potential probe of hydrophobicity in biological systems.

Conclusions

The inclusion of the $BP(OH)_2$ molecule inside CDs and HSA was studied using absorption and fluorescence spectroscopy. The stoichiometric ratios and the binding constants of the complexes were deduced by fitting the changes in the spectral intensity to BH and NLR algorithms. It was found that the stoichiometry of the $BP(OH)_2$/(α-CD) complex is dominated by 1:2, whereas in all other CDs and in HSA this ratio is 1:1. The structure of the $BP(OH)_2$:(α-CD)$_2$ complex was calculated using ab initio methods at the HF/STO-3G level, and the optimum geometry indicates that the inclusion of the $BP(OH)_2$ molecule is axial and centered between the two cavities of α-CDs. The $BP(OH)_2$ molecule maintains its DE moiety with

no possible hydrogen bonding with the host interior H-atoms. Analysis of these results along with the inclusion of $BP(OH)_2$ in four other CDs indicates that absorption and fluorescence of $BP(OH)_2$ are very sensitive to the change in the cavity size of CD and its hydrophobicity.

Binding of $BP(OH)_2$ to HSA was examined in order to test the applicability of $BP(OH)_2$ as a microenvironment-sensitive probe in biology. The changes in both the absorption and fluorescence spectra of $BP(OH)_2$ upon the addition of HSA indicate that $BP(OH)_2$ binds to subdomain IIA in HSA which is characterized by hydrophobic interactions.

The results presented here suggest that the $BP(OH)_2$ molecule represents a potentially useful new photophysical probe in biological and inclusion studies.

Acknowledgment. This work was supported by the Sultan Qaboos University (Grant No. IG/SCI/CHEM/05/03).

References and Notes

(1) Royer, C. A. *Chem. Rev.* **2006**, *106*, 1769.
(2) Neyroz, P.; Franzoni, L.; Menna, C.; Spisni, A.; Masotti, L. *J. Fluoresc.* **1996**, *6*, 127.
(3) Sytnik, A.; Gormin, D.; Kasha, M. *Proc. Natl. Acad. Sci. U.S.A.* **1994**, *91*, 11968.
(4) Sytnik, A.; Kasha, M. *Proc. Natl. Acad. Sci. U.S.A.* **1994**, *91*, 8627.
(5) Sytnik, A.; Litvinyuk, Y. *Proc. Natl. Acad. Sci. U.S.A.* **1996**, *93*, 12959.
(6) Bulska, H. *Chem. Phys. Lett*. **1983**, *98*, 398.
(7) Bulska, H.; Grabowska, A.; Grabowski, Z. R. *J. Lumin*. **1986**, *35*, 189.
(8) Sepiol, J.; Bulska, H.; Grabowska, A. *Chem. Phys. Lett*. **1987**, *140*, 607.
(9) Kaschke, M.; Rentsch, S.; Opfermann, J. *Laser Chem.* **1988**, *8*, 377.
(10) Sepiol, J.; Grabowska, A.; Bulska, H.; Mordzinski, A.; Perez Salgado, F.; Rettschnick, R. P. H. *Chem. Phys. Lett.* **1989**, *163*, 443.
(11) Wortmann, R.; Elich, K.; Lebus, S.; Liptay, W.; Borowicz, P. *J. Phys. Chem.* **1992**, *96*, 9724.
(12) Borowicz, P.; Grabowska, A.; Wortmann, R.; Liptay, W. *J. Lumin.* **1992**, *52*, 265.
(13) Zhang, H.; van der Meulen, P.; Glasbeek, M. *Chem. Phys. Lett.* **1996**, *253*, 97.
(14) Marks, D.; Prosposito, P.; Zhang, H.; Glasbeek, M. *Chem. Phys. Lett.* **1998**, *289*, 535.
(15) Prosposito, P.; Marks, D.; Zhang, H.; Glasbeek, M. *J. Phys. Chem. A* **1998**, *102*, 8894.
(16) Marks, D.; Zhang, H.; Glasbeek, M.; Borowicz, P.; Grabowska, A. *Chem. Phys. Lett.* **1997**, *275*, 370.
(17) Toele, P.; Zhang, H.; Glasbeek, M. *J. Phys. Chem. A* **2002**, *106*, 3651.
(18) Barone, V.; Adamo, C. *Chem. Phys. Lett.* **1995**, *241*, 1.
(19) Sobolewski, A. L.; Adamowicz, L. *Chem. Phys. Lett.* **1996**, *252*, 33.
(20) Barone, V.; Palma, A.; Sanna, N. *Chem. Phys. Lett.* **2003**, *381*, 451.
(21) Gelabert, R. R.; Moreno, M.; Lluch, J. M. *ChemPhysChem* **2004**, *5*, 1372.
(22) Lipkowski, J.; Grabowska, A.; Waluk, J.; Calestani, G.; Hess, B. A. *J. Crystallogr. Spectrosc. Res.* **1992**, *22*, 563.
(23) Abou-Zied, O. K. *J. Photochem. Photobiol., A* **2006**, *182*, 192.
(24) Abou-Zied, O. K; Al-Hinai, A. T. *J. Phys. Chem. A* **2006**, *110*, 7835.
(25) Berde, C. B.; Hudson, B. S.; Simon, R. D.; Sklar, L. A. *J. Biol. Chem.* **1979**, *254*, 391.
(26) He, X. M.; Carter, D. C. *Nature* **1992**, *358*, 209.
(27) Bhattacharya, A. A.; Curry, S.; Franks, N. P. *J. Biol. Chem.* **2000**, *275*, 38731.
(28) Gellman, H. S. (Ed.) *Chem. Rev.* **1997**, *97*, 1231.
(29) Wallevik, K. *J. Biol. Chem.* **1973**, *248*, 2650.
(30) Schmidt, M. W.; Baldridge, K. K.; Boatz, J. A.; Elbert, S. T.; Gordon, M. S.; Jensen, J. H.; Koseki, S.; Matsunaga, N.; Nguyen, K. A.; Su, S. J.; Windus, T. L.; Dupuis, M.; Montgomery, J. A. *J. Comput. Chem.* **1993**, *14*, 1347.
(31) Carballeira, L.; Perez-Juste, I. *THEOCHEM* **1996**, *368*, 17.
(32) Benesi, A. H.; Hildebrand, J. H. *J. Am. Chem. Soc*. **1949**, *71*, 2703.
(33) Abou-Zied, O. K. *Spectrochim. Acta, Part A* **2005**, *62*, 245.
(34) Connors, K. A. *Binding Constants. The Measurements of Molecular Complex Stability*; Wiley: New York, 1987.
(35) Mwalupindi, A. G.; Rideau, A.; Agbaria, R. A.; Warner, I. M. *Talanta* **1994**, *41*, 599.
(36) (a) Mitra, S.; Das, R.; Mukherjee, S. *J. Phys. Chem. B* **1998**, *102*, 3730. (b) Roberts, E. L.; Dey, J.; Warner, I. M. *J. Phys. Chem.* **1996**, *100*, 19681.
(37) Hamai, S. *J. Phys. Chem. B* **1997**, *101*, 1707.
(38) Dos Santos, H. F.; Duarte, H. A.; Sinisterra, R. D.; Mattos, S. V. D.; De Oliveira, L. F. C.; De Almeida, W. B. *Chem. Phys. Lett.* **2000**, *319*, 569.
(39) Nascimento, C. S.; Dos Santos, H. F.; De Almeida, W. B. *Chem. Phys. Lett.* **2004**, *397*, 422.
(40) Bea, I.; Gotsev, M. G.; Ivanov, P. M.; Jaime, C.; Kollman, P. A. *J. Org. Chem.* **2006**, *71*, 2056.
(41) Ivanov, P. M.; Jaime, C. *J. Phys. Chem. B* **2004**, *108*, 6261.
(42) Ivanov, P. M.; Jaime, C. *J. Mol. Struct.* **1996**, *377*, 137.
(43) Ivanov, P. M.; Jaime, C. *An. Quim.* **1996**, *92*, 13.
(44) Chacko, K. K.; Saenger, W. *J. Am. Chem. Soc.* **1981**, *103*, 1708.
(45) Jensen, F. *Introduction to Computational Chemistry*; Wiley: New York, 1999.
(46) Bender, M. L.; Komiyama, M. *Cyclodextrin Chemistry*; Springer: Berlin, 1978.
(47) Szejtli, J. *Cyclodextrins and their Inclusion Complexes*; Akadémiai Kiadó: Budapest, 1982.
(48) Easton, C. J.; Lincoln, S. F. *Modified Cyclodextrins: Scaffolds and Templates for Supramolecular Chemistry*; Imperial College: London, 1999.
(49) Information available from the supplier (Fluka) indicates that the degree of methyl substitution is 1.7−1.9 CH_3 per unit of anhydroglucose. The available molecular structure does not indicate the positions of the methyl groups in the molecule. The molecular weight of Mβ-CD is not mentioned on the Fluka product, but the average molecular weight is mentioned on the Aldrich product to be 1310 g mol^{-1}.
(50) Reichardt, C. *Solvents and Solvent Effects in Organic Chemistry*; VCH: Weinheim, 1988.
(51) Madrid, J. M.; Mendicuti, F.; Mattice, W. L. *J. Phys. Chem. B* **1998**, *102*, 2037.
(52) Funasaki, N.; Ishikawa, S.; Neya, S. *J. Pharm. Sci.* **2001**, *90*, 740.